Hindawi Publishing Corporation
Abstract and Applied Analysis
Volume 2012, Article ID 835304, 15 pages
doi:10.1155/2012/835304

Research Article

A Chaotic Pulse-Time Modulation Method for Digital Communication

Nguyen Xuan Quyen, Vu Van Yem, and Thang Manh Hoang

School of Electronics and Telecommunications, Hanoi University of Science and Technology, 1 Dai Co Viet, Hanoi, Vietnam

Correspondence should be addressed to Thang Manh Hoang, thang@ieee.org

Received 15 January 2012; Revised 6 March 2012; Accepted 6 March 2012

Academic Editor: Muhammad Aslam Noor

We present and investigate a method of chaotic pulse-time modulation (PTM) named chaotic pulse-width-position modulation (CPWPM) which is the combination of pulse-position-modulation (PPM) and pulse-width modulation (PWM) with the inclusion of chaos technique for digital communications. CPWPM signal is in the pulse train format, in which binary information is modulated onto chaotically-varied intervals of position and width of pulses, and therefore two bits are encoded on a single pulse. The operation of the method is described and the theoretical evaluation of bit-error rate (BER) performance in the presence of additive white Gaussian noise (AWGN) is provided. In addition, the chaotic behavior with tent map and its effect on average parameters of the system are investigated. Theoretical estimation and numerical simulation of a CPWPM system with specific parameters are carried out in order to verify the performance of the proposed method.

1. Introduction

In recent years, chaotic behavior has been investigated in various research fields such as physics, biology, chemistry, and engineering [1]. Chaos-based digital communication has been receiving significant attention [2] due to its potentials in improving the privacy of information [3]. Many chaos-based modulation methods have been proposed using different modulation schemes [3, 4]. Each method has its own advantages and disadvantages but most of them use the chaotic carrier created by a chaotic dynamical system to convey information, so they are sensitive to distortion and noise that can strongly affect the synchronization [5–7] and cause errors in recovering information.

Pulse-time modulation (PTM) technique was reported in the last 1940s [8] and it has received significant attention for the development of digital communication, especially with

optical fiber transmission system. In PTM, the binary information is modulated onto one of time-dependent parameters such as position, width, interval, or frequency in order to create the corresponding methods which are pulse-position modulation (PPM), pulse-width modulation (PWM), pulse-interval modulation (PIM) or pulse-frequency modulation (PFM) [9].

A chaotic PTM method named chaotic-pulse-position modulation (CPPM) was proposed [10, 11] to reduce the effect of the channel on chaos synchronization. Since binary information is only modulated onto the interpulse intervals, the impact of distortion and noise on the pulse shape does not seriously affect the synchronization process. The principal advantage of CPPM is the automatic synchronization with the noncoherent demodulation type and without the need of specific hand-shaking protocols [12].

In this research, we present and investigate a method named chaotic-pulse-position-width modulation (CPWPM) which is the combination of PPM and PWM with the inclusion of chaos technique. In which, the binary information is modulated onto two chaotically-varied intervals that are position and width of pulses. The position and width of a pulse are determined by time intervals from its rising edge to the previous rising edge and to its falling edge, respectively. With each received pulse, the binary information of two bits are recovered and thus transmission rate can be improved. Since the CPWPM signal also has the pulse train format which guides the synchronization in an automatic way, so this method performs well in distortion- and noise-affected channels as well as achieves a high level of information privacy.

The rest of this paper is organized as follows: the operation of the CPWPM method is described in Section 2. Section 3 presents the theoretical evaluation of the BER performance in AWGN channel. In Section 4, we investigate the chaotic behavior of CPWPM with tent map, from that average parameters of the system are determined. A CPWPM system with specific parameters is calculated and simulated, and their results are shown in Section 5. Finally, concluding remarks are given in Section 6.

2. Description of CPWPM

In this section we describe operation of the CPWPM method by means of the analysis of modulation and demodulation schemes which are illustrated in Figures 1(a) and 1(b), respectively. Basically, each scheme is built around a chaotic pulse regenerator (CPRG) as shown in Figure 2.

2.1. CPRG

In the CPRG, a counter operates in free running mode to produce a linearly increasing signal, $C(t) = K_1 t$, where t is the time duration from the reset instance and K_1 is count-step (the slope of the signal). This linearly increasing signal is reset to zero by the input pulse. Before the reset time, t_n, the output value of the counter, $X_n^1 = K_1 \Delta T_n$, is stored in the sample-and-hold circuit $(S + H)$ whose output is fed to the nonlinear converter, $F(\cdot)$. An amplifier with a gain-factor, $K > 1$, is used to produce another linearly increasing signal, $A(t) = KK_1 t = K_2 t$, which has a higher slope compared with that of the input signal. When the magnitude of the output signal of the amplifier and that of counter reach the same value $F(X_n^1)$ at the output of the $F(\cdot)$, two narrow pulses at Outputs 2 and 1 are generated at the times, $t_n^2 = t_n + F(X_n^1)/K_2$ and $t_n^1 = t_n + F(X_n^1)/K_1$, respectively. It is easy to see that the time t_n^2 is earlier than t_n^1 and

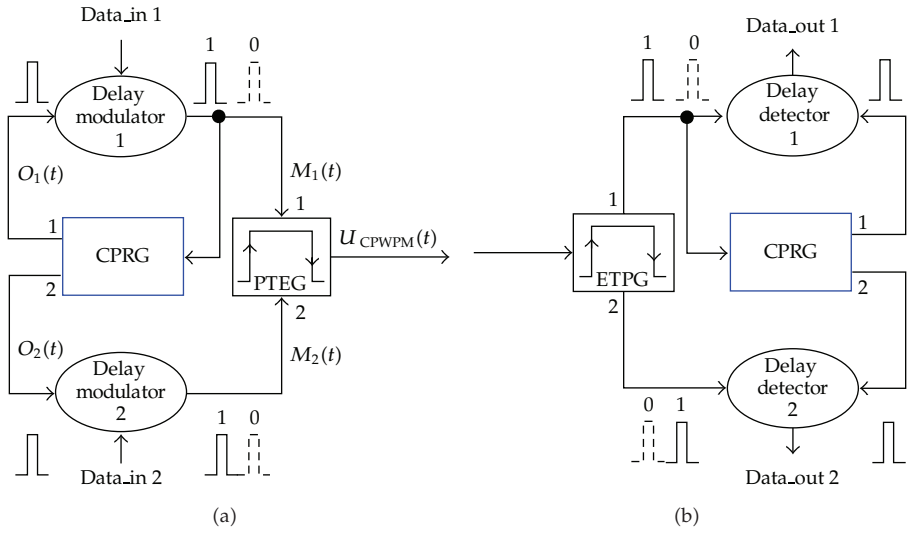

Figure 1: (a) Modulation scheme, (b) demodulation scheme.

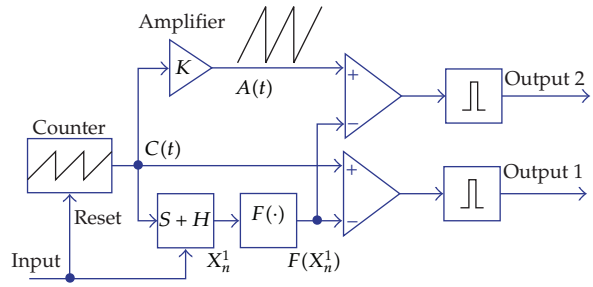

Figure 2: Scheme for the CPRG.

these times can be controlled by the values of the gain-factor K and count-step K_1. With a proper choice of parameters, when Output 1 is connected back to the input to form a closed loop, CPRG will generate two chaotic pulse trains at its two outputs.

2.2. Modulation

In the modulation scheme, the binary information is modulated separately onto the interpulse intervals of two consecutive pulses at the outputs of CPRG by using delay modulators in the corresponding feedback loops. At the delay modulators, the input pulses trigger data source to get the next binary bits S_n^2 and S_{n+1}^1. Depending on the values of these binary bits, the input pulses, $O_2(t)$ and $O_1(t)$, are delayed by time durations, $d_2 + m_2 S_n^2$ and $d_1 + m_1 S_{n+1}^1$, respectively. Note that d_1 and d_2 are constant time delays inserted to guarantee the synchronization of the system, m_1 and m_2 are modulation depths which are delayed-time differences between "0" and "1" bits. Therefore, the delayed pulses $M_2(t)$ and $M_1(t)$ at the outputs of the delay modulators 2 and 1 are generated at the times, $t_n^* = t_n^2 + d_2 + m_2 S_n^2$ and $t_{n+1} = t_n^1 + d_1 + m_1 S_{n+1}^1$, respectively. After that, the modulated chaotic pulse trains are

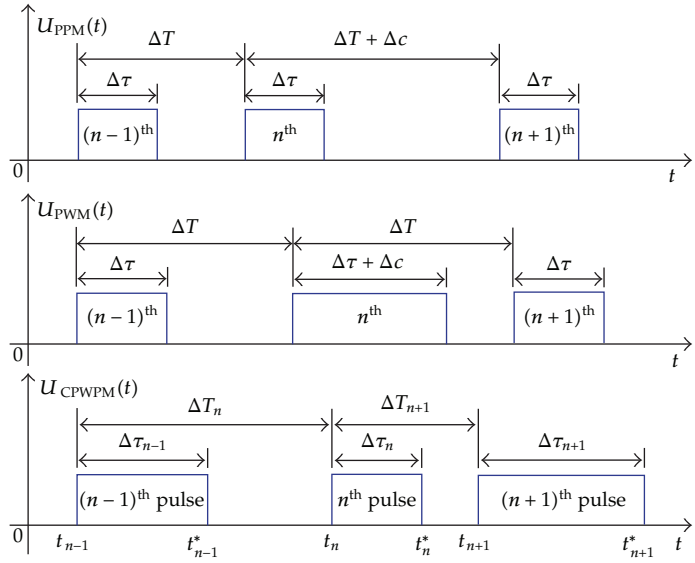

Figure 3: Illustration of the PPM, PWM, and CPWPM signals.

applied to a pulse-triggered edge generator (PTEG) whose output will switch to high and low levels as triggering by the inputs, $M_1(t)$ and $M_2(t)$, to define the position and width of pulses, respectively. The pulse train at the output of PTEG is the CPWPM signal which is mathematically expressed as follows:

$$U_{\mathrm{CPWPM}}(t) = \sum_{n=0}^{\infty} A[u(t - t_n) - u(t - t_n - \Delta\tau_n)], \tag{2.1}$$

where $u(t)$ is the unit-step function, t_n is the time to generate the nth pulse, and A and $\Delta\tau_n$ are the amplitude and width of pulses, respectively. It is clear that the width of the nth pulse and the position of the $(n+1)$th pulse are determined by the following intervals:

$$\begin{aligned} \Delta\tau_n &= \frac{F(K_1\Delta T_n)}{K_2} + d_2 + m_2 S_n^2, \\ \Delta T_{n+1} &= \frac{F(K_1\Delta T_n)}{K_1} + d_1 + m_1 S_{n+1}^1. \end{aligned} \tag{2.2}$$

The comparison between the PPM, PWM, and CPWPM signals in the time domain is illustrated in Figure 3. In the conventional PPM, the binary information is modulated onto interpulse interval (interval of inter-rising edge) which determines the position of the current pulse compared to the previous pulse, while the width of pulses $\Delta\tau$ is fixed. In contrast, in the PWM method, the interpulse intervals ΔT are fixed, and the information is modulated onto the pulse widths (interval of rising and falling edges of a same pulse). With the PPM and PWM methods, time difference between modulated intervals of "0" and "1" bits is a constant Δc. In our proposed method CPWPM, both the interpulse interval ΔT_n and the width $\Delta\tau_n$ of pulses convey the binary information and their variation is controlled by the

nonlinear function $F(\cdot)$. This can be seen from the expression in (2.2). Values of parameters $m_1, m_2, d_1, d_2, K_1, K$, and $F(\cdot)$ are chosen so that chaotic behavior exhibits in (2.2), in other words, the position and width of CPWPM pulses vary chaotically.

2.3. Demodulation

In the demodulation scheme, the received signal is applied to an edge-triggered pulse generator (ETPG). ETPG is triggered by the rising and falling edges of input pulses to produce narrow pulses at Outputs 1 and 2, respectively. Output 1 of ETPG is connected to CPRG which is identical as in the modulation scheme. As the synchronization state is maintained, the reproduced chaotic pulse trains at the outputs of CPRG are identical to those in the modulation scheme. At Delay detectors 1 and 2, these pulses are compared with the corresponding ones from ETPG to determine the delayed-time durations, $\Delta\tau_n - F(C_n)/K_2$ and $\Delta T_{n+1} - F(C_n)/K_1$, respectively. Consequently, data bits are recovered as follows:

$$\begin{aligned} S_n^2 &= \frac{(\Delta\tau_n - (F(K_1\Delta T_n)/K_2) - d_2)}{m_2}, \\ S_{n+1}^1 &= \frac{(\Delta T_{n+1} - (F(K_1\Delta T_n)/K_1) - d_1)}{m_1}. \end{aligned} \tag{2.3}$$

Like CPPM, the CPWPM system can automatically synchronize due to its pulse train format. Equation (2.3) points out that the demodulation scheme only needs to correctly detect three consecutive intervals, ΔT_n, $\Delta\tau_n$ and ΔT_{n+1}, in order to resynchronize and decode correctly. Note that the set of values of $m_1, m_2, d_1, d_2, K_1, K$ and $F(\cdot)$ is considered as a secret key. The binary information is only correctly recovered when a receiver has full information on these parameters.

Since two data bits are recovered with each received pulse, the bit rate of transmission is twice improved in comparison with PPM, PWM, and CPPM. Furthermore, data bits at the inputs (i.e., Data_ins 1 and 2) in the modulation scheme are recovered separately at their corresponding outputs (i.e., Data_outs 1 and 2) in the demodulation scheme. Therefore, CPWPM can provide a multiaccess method of two users.

3. Theoretical Evaluation of BER Performance

The analytical method to evaluate the CPPM error probability reported in [11] is employed for evaluating the BER of CPWPM in this research. For simplicity, let us consider a system model presented in Figure 4. The input signal of the threshold detector, $y(t)$, is the sum of the transmitted signal and channel noise (AWGN), and it is compared with a threshold value H. When the magnitude of $y(t)$ changes over H, corresponding edges are produced and thus a rectangular pulse $p(t)$ with an amplitude A is regenerated at the output. The resulting pulse train of $p(t)$ is put into the CPWPM demodulator for recovering the data information.

The detection windows of the rising and falling edges of the nth pulse in the demodulator are defined as in Figure 5. Assumed that the demodulator maintains the synchronization at all times, the reproduced pulse trains at the outputs of CPRG are identical to those in the modulator, and therefore the instances t_{n-1}^1 and t_n^2 are determined. The rising and falling edge detection durations are taken from $(t_{n-1}^1 + d_1)$ to $(t_{n-1}^1 + d_1 + m_1)$ and from $(t_n^2 + d_2)$ to $(t_n^2 + d_2 + m_2)$, respectively. The width of each detection duration is equal to the

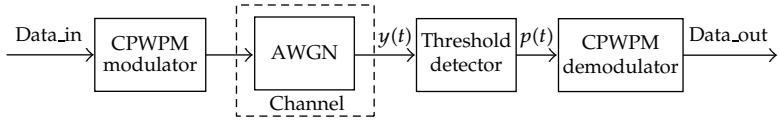

Figure 4: Simplified model of a CPWPM system.

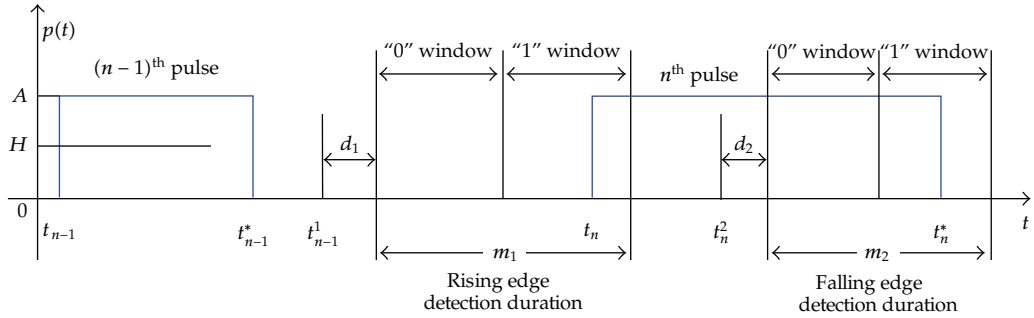

Figure 5: Detection windows of the nth pulse in the CPWPM demodulator.

corresponding modulation depth and it is divided into "0" and "1" windows, both have the same width. Due to the effect of noise on the signal $y(t)$, bit error will occur when the shifted pulse edges of the pulse train $p(t)$ fall into unexpected windows in the corresponding detection durations. It means that the pulse edges of the pulse $p(t)$ of transmitted "0" bits fall into "1" windows and vice versa. Here, we divide each window into bins; each bin has the width τ which is also the fundamental sampling period of the system. It is noted that $1/\tau$ is frequency of clock pulse supplying to Counter in CPRG at the demodulator. The signal $y(t)$ is sampled once at the end of every bin with sampling cycle τ.

Each CPWPM pulse is equivalent to one symbol from S_{00}, S_{01}, S_{10}, or S_{11} which carries the binary information of two bits from "00", "01", "10" or "11", respectively. We consider the case that the symbol S_{11} is transmitted and the correct detection probability of this symbol is

$$P\left(\frac{c}{S_{11}}\right) = P_{11/11} = P_{R1/1} \times P_{F1/1}, \tag{3.1}$$

where $P_{R1/1}$ and $P_{F1/1}$ are the probabilities to detect "1" bit when "1" bit is transmitted in the rising and falling edge detection durations, respectively. Let us first evaluate $P_{R1/1}$ which is the probability of the signal $y(t)$ from any bin in the "0" window not exceeding the threshold value H. Using the statistical independence of the measurements for each window in the case of AWGN, we have

$$P_{R1/1} = \prod_{i=1}^{m_1/2\tau} \left[P_i(y_i < H)\right] = \left[P(y < H)\right]^{m_1/2\tau}$$

$$= \left[\frac{1}{\sqrt{2\pi\sigma^2}}\int_{-\infty}^{H}\exp\left(-\frac{x^2}{2\sigma^2}\right)dx\right]^{m_1/2\tau}$$
$$= \left[\frac{1}{2}\operatorname{erfc}\left(-\frac{H}{\sqrt{2\sigma^2}}\right)\right]^{m_1/2\tau} = \left[\frac{1}{2}\operatorname{erfc}\left(-h\sqrt{\frac{E_b}{N_o}}\right)\right]^{m_1/2\tau}. \tag{3.2}$$

Secondly, we evaluate $P_{F1/1}$ which is the probability of the signal $y(t)$ from any bin in the "0" window which remains higher than the threshold value H. Thus, it is determined as follows:

$$P_{F1/1} = \prod_{i=1}^{m_2/2\tau}\left[P_i(y_i > H)\right] = \left[P(y > H)\right]^{m_2/2\tau}$$
$$= \left[\frac{1}{\sqrt{2\pi\sigma^2}}\int_{H}^{+\infty}\exp\left(-\frac{(x-A)^2}{2\sigma^2}\right)dx\right]^{m_2/2\tau} \tag{3.3}$$
$$= \left[\frac{1}{2}\operatorname{erfc}\left(\frac{H-A}{\sqrt{2\sigma^2}}\right)\right]^{m_2/2\tau} = \left[\frac{1}{2}\operatorname{erfc}\left((h-1)\sqrt{\frac{E_b}{N_o}}\right)\right]^{m_2/2\tau}.$$

In (3.2) and (3.3), $m_1/2$ and $m_2/2$ are the window widths in the rising and falling edge detection durations, respectively; the rate $h = H/A$; $E_b = A^2\tau$ and $N_o = 2\sigma^2\tau$ are the energy per bit and the spectrum power density of noise, respectively.

The recovery will be unsuccessful if at least one of four symbols is decoded incorrectly. From (3.1), (3.2), and (3.3), the error probability of CPWPM can be estimated by the following equation:

$$\begin{aligned}\mathrm{BER}_{\mathrm{CPWPM}} &= 1 - P\left(\frac{c}{S_{11}}\right) = 1 - P_{R1/1}\times P_{F1/1}\\ &= 1 - \left[\frac{1}{2}\operatorname{erfc}\left(-h\sqrt{\frac{E_b}{N_o}}\right)\right]^{m_1/2\tau}\times\left[\frac{1}{2}\operatorname{erfc}\left((h-1)\sqrt{\frac{E_b}{N_o}}\right)\right]^{m_2/2\tau}.\end{aligned} \tag{3.4}$$

4. Chaotic Behavior with Tent Map and Average Parameters

Tent map is a discrete-time and one-dimension nonlinear function with the piecewise-linear I/O characteristic curve [13] and it is used for generating chaotic values seen as pseudorandom numbers [14]. In the communication, the tent map is proposed for application in chaotic modulation [15] with such advantages as the simplified calculation and the robust regime of chaos generation for rather broad range of modulation parameters. Here, the utilization of tent map for chaotic behavior of CPWPM is investigated. Based on average fixed point of the map, average parameters of the CPWPM system are determined theoretically. These are very important for design process to guarantee the chaotic behavior in the system.

4.1. CPWPM Tent Map

The conventional tent map is iteratively generated through a transformation function $F(\cdot) : [0,1] \rightarrow [0,1]$ as given by

$$x_n = F(x_n) = F^{n-1}(x_0) = \begin{cases} ax_{n-1}, & 0 \le x_{n-1} \le 0.5, \\ a(1 - x_{n-1}), & 0.5 < x_{n-1} \le 1. \end{cases} \tag{4.1}$$

In this equation, n represents the time step; x_0 is the initial value; x_{n-1} is the output value at the nth step, and the parameter a controls the chaotic behavior of the map.

In CPWPM, from (2.2), the position and width of the nth pulse are rewritten as follows:

$$\begin{aligned} \Delta T_n &= \frac{F(K_1 \Delta T_n - 1)}{K_1} + d_1 + m_1 S_n^1, \\ \Delta \tau_n &= \frac{F(K_1 \Delta T_n)}{K_2} + d_2 + m_2 S_n^2, \end{aligned} \tag{4.2}$$

then these intervals can be converted to the following:

$$\begin{aligned} \underbrace{K_1 \Delta T_n}_{X_n^1} &= F\underbrace{(K_1 \Delta T_{n-1})}_{X_{n-1}^1} + \underbrace{K_1 d_1}_{d_1^*} + \underbrace{K_1 m_1}_{m_1^*} S_n^1, \\ \underbrace{K_2 \Delta \tau_n}_{X_n^2} &= F\underbrace{(K_1 \Delta T_n)}_{X_n^1} + \underbrace{K_2 d_2}_{d_2^*} + \underbrace{K_2 m_2}_{m_2^*} S_n^2, \end{aligned} \tag{4.3}$$

here, $K_1 \Delta T_{n-1}$, $F(K_1 \Delta T_{n-1})$, and $K_1 \Delta T_n$, $F(K_1 \Delta T_n)$ are the input and output values of the nonlinear converter $F(\cdot)$ at the $(n-1)$th and nth steps, respectively. After that, we have

$$\begin{aligned} X_n^1 &= F\left(X_{n-1}^1\right) + d_1^* + m_1^* S_n^1, \\ X_n^2 &= F\left(X_n^1\right) + d_2^* + m_2^* S_n^2. \end{aligned} \tag{4.4}$$

From (4.1) and (4.4), the tent map for the CPWPM system, called the CPWPM ten map, is derived as

$$\begin{aligned} X_n^1 = F_1\left(X_{n-1}^1\right) &= \begin{cases} aX_{n-1}^1 + d_1^* + m_1^* S_n^1, & 0 \le X_{n-1}^1 \le 0.5, \\ a\left(1 - X_{n-1}^1\right) + d_1^* + m_1^* S_n^1, & 0.5 < X_{n-1}^1 \le 1, \end{cases} \\ X_n^2 = F_2\left(X_n^1\right) &= \begin{cases} aX_n^1 + d_2^* + m_2^* S_n^2, & 0 \le X_n^1 \le 0.5, \\ a\left(1 - X_n^1\right) + d_2^* + m_2^* S_n^2, & 0.5 < X_n^1 \le 1. \end{cases} \end{aligned} \tag{4.5}$$

4.2. Chaotic Behavior

The equation of the CPWPM tent map above points out that its chaotic behavior depends on not only the control parameter a, but also on the parameters $\delta_1 = d_1^* + m_1^* S_n^1$ and $\delta_2 = d_2^* + m_2^* S_n^2$.

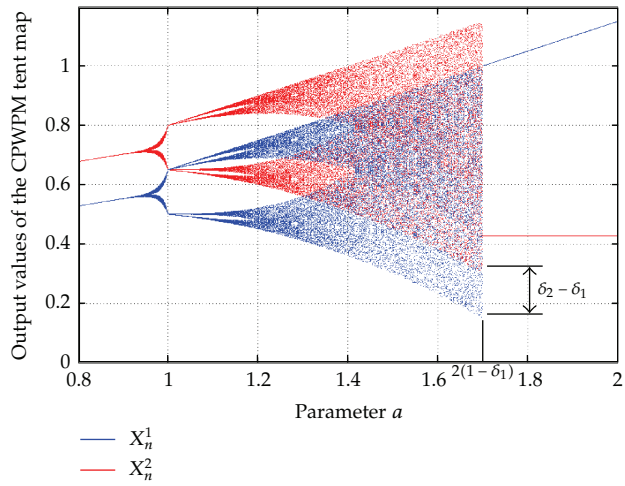

Figure 6: Bifurcation diagram of the CPWPM tent map.

The chaos of X_n^1 depends on a and δ_1; the chaos of X_n^2 depends on the chaos of X_n^1 with a difference, $X_n^2 - X_{n+1}^1 = \delta_2 - \delta_1$. In other words, the chaos of X_n^1 leads to the chaos of the system.

The Lyapunov exponent of the map is determined by

$$\lambda = \lim_{k\to\infty}\left(\frac{1}{k}\sum_{n=0}^{k-1}\ln\left|\frac{dF_1(X_n^1)}{dX_n^1}\right|\right) = \lim_{k\to\infty}\left(\frac{1}{k}\sum_{n=0}^{k-1}\ln a\right) = \ln a. \tag{4.6}$$

Based on (4.5) and (4.6), the behavior of the CPWPM tent map becomes chaotic in $[0,1]$ with the following condition:

$$\begin{aligned} \delta_1 &\geq 0, \\ 0.5a + \delta_1 &\leq 1, \\ \lambda = \ln a &> 0, \end{aligned} \tag{4.7}$$

which is equivalent to

$$\begin{aligned} 0 \leq \delta_1 &\leq 0.5, \\ 1 < a &\leq 2(1-\delta_1). \end{aligned} \tag{4.8}$$

Figure 6 shows the bifurcation diagram of the CPWPM tent map according to a and δ_1, δ_2. Here, $\delta_1 = 0$ is as the conventional tent map; the more the value of δ_1 increases, the smaller the chaotic area is. And, in the $\delta_1 > 0.5$ the chaotic area disappears. It is easy to find that the bifurcation diagram of X_n^2 is also the bifurcation diagram of X_n^1 after being shifted vertically with a distance, $\delta_2 - \delta_1$.

In the modulation process, the binary bit S_n^1 varies between "0" or "1" and thus δ_1 has two values, d_1^* and $d_1^* + m_1^*$. Based on (4.8), *the condition* in order to guarantee the chaotic behavior in the CPWPM method are

$$\begin{aligned} 0 &\le m_1^* + d_1^* \le 0.5, \\ 1 &\le a \le 2\left(1 - \left(m_1^* + d_1^*\right)\right), \end{aligned} \tag{4.9}$$

or

$$\begin{aligned} &0 \le K_1(m_1 + d_1) \le 0.5, \\ &1 \le a \le 2(1 - K_1(m_1 + d_1)). \end{aligned} \tag{4.10}$$

4.3. Average Parameters

In the iteration process, the CPWPM tent map varies chaotically around a fixed point [1] $(X_{\text{fp}}^1, X_{\text{fp}}^2)$ determined by

$$\begin{aligned} X_{\text{fp}}^1 &= F_1\left(X_{\text{fp}}^1\right) = \frac{a + \delta_1}{1 + a}, \\ X_{\text{fp}}^2 &= F_2\left(X_{\text{fp}}^1\right) = \frac{a(1 - \delta_1)}{1 + a} + \delta_2. \end{aligned} \tag{4.11}$$

In the modulation process, due to the variation between "0" or "1" of input binary bits S_n^1 and S_n^2, this fixed point is shifted around an average fixed point $(X_{\text{av}}^1, X_{\text{av}}^2)$ as follows:

$$\begin{aligned} X_{\text{av}}^1 &= \frac{a + (d_1 + m_1/2)}{1 + a}, \\ X_{\text{av}}^2 &= \frac{a(1 - (d_1 + m_1/2))}{1 + a} + d_2 + \frac{m_2}{2}. \end{aligned} \tag{4.12}$$

Due to this feature, the intervals of position and width of the CPWPM signal vary chaotically around average intervals:

$$\begin{aligned} \Delta T_{\text{av}} &= \lim_{k \to \infty} \left(\frac{1}{k} \sum_{n=0}^{k} \Delta T_n \right) \approx \frac{X_{\text{av}}^1}{K_1}, \\ \Delta \tau_{\text{av}} &= \lim_{k \to \infty} \left(\frac{1}{k} \sum_{n=0}^{k} \Delta \tau_n \right) \approx \frac{X_{\text{av}}^2}{K_2}, \end{aligned} \tag{4.13}$$

and its spectrum therefore has an average fundamental harmonic $f_{\text{av–fund}}$ and an average bandwidth BW_{av} which are

$$\begin{aligned} f_{\text{av–fund}} &= \frac{1}{\Delta T_{\text{av}}} \approx \frac{K_1}{X_{\text{av}}^1}, \\ \text{BW}_{\text{av}} &= \frac{1}{\Delta \tau_{\text{av}}} \approx \frac{K_2}{X_{\text{av}}^2}. \end{aligned} \tag{4.14}$$

The value of the average fundamental harmonic is equal to the average number of pulses transmitted in one second. Since each CPWPM pulse conveys two bits, the average bit-rate $\mathrm{BR}_{\mathrm{av}}$ of the system is evaluated as follows:

$$\mathrm{BR}_{\mathrm{av}} = 2 \times f_{\mathrm{av-fund}} \approx \frac{2K_1}{X_{\mathrm{av}}^1}. \tag{4.15}$$

5. Calculation and Simulation Results

In this section, the CPWPM system as the model in Figure 4 with specific parameters is calculated theoretically and simulated numerically in order to verify the analysis and performance of the presented method. The estimation and simulation results as well as comparison are provided. The specific parameters of the CPWPM system are chosen as follows: the fundamental sampling period $\tau = 1\,\mu$s, $K_1 = 0.002/\mu$s, $K = 2.5$, $d_1 = 20\,\mu$s, $d_2 = 10\,\mu$s, $m_1 = 50\,\mu$s, $m_2 = 30\,\mu$s, $H = 0.5$, $A = 1$; the nonlinear converter $F(\cdot)$ uses the tent map with $a = 1.5$.

5.1. Theoretical Calculation

Based on (4.3), the CPWPM tent map is determined by the following parameters:

$$\begin{aligned}
&K_2 = KK_1 = (0.002/\mu\mathrm{s}) \times 2.5 = 0.005/\mu\mathrm{s}, \qquad d_1^* = K_1 d_1 = (0.002/\mu\mathrm{s}) \times 20\,\mu\mathrm{s} = 0.04,\\
&d_2^* = K_2 d_2 = (0.005/\mu\mathrm{s}) \times 10\,\mu\mathrm{s} = 0.05, \qquad m_1^* = K_1 m_1 = (0.002/\mu\mathrm{s}) \times 50\,\mu\mathrm{s} = 0.1,\\
&m_2^* = K_2 m_2 = (0.005/\mu\mathrm{s}) \times 30\,\mu\mathrm{s} = 0.15,\\
&K_1(d_1 + m_1) = (0.002/\mu\mathrm{s}) \times (20\,\mu\mathrm{s} + 50\,\mu\mathrm{s}) = 0.14.
\end{aligned} \tag{5.1}$$

With $K_1(d_1 + m_1) = 0.14$, the condition for the chaos of the method according to (4.10) becomes $1 < a \leq 2(1 - 0.14) = 1.72$. Therefore, we choose $a = 1.5$ to guarantee the chaotic behavior of the CPWPM system. Based on the analysis in the Section 4.3, the average parameters of the system are calculated as follows:

$$\begin{aligned}
&X_{\mathrm{av}}^1 = \frac{1.5 + (0.04 + 0.1/2)}{1 + 1.5} = 0.636, \qquad X_{\mathrm{av}}^2 = \frac{1.5(1 - (0.04 + 0.1/2))}{1 + 1.5} + 0.05 + \frac{0.15}{2} = 0.671,\\
&\Delta T_{\mathrm{av}} \approx \frac{X_{\mathrm{av}}^1}{K_1} = \frac{0.636}{0.002} = 318\,\mu\mathrm{s}, \qquad \Delta\tau_{\mathrm{av}} \approx \frac{X_{\mathrm{av}}^2}{K_2} = \frac{0.671}{0.005} = 134.2\,\mu\mathrm{s},\\
&f_{\mathrm{av-fund}} = \frac{1}{\Delta T_{\mathrm{av}}} \approx \frac{1}{318} = 3.145\,\mathrm{kHz}, \qquad \mathrm{BW}_{\mathrm{av}} = \frac{1}{\Delta\tau_{\mathrm{av}}} \approx \frac{1}{134} = 7.451\,\mathrm{kHz},\\
&\mathrm{BR}_{\mathrm{av}} = 2 \times f_{\mathrm{av-fund}} \approx 2 \times 3.145 = 6.29\,\mathrm{Kbps}.
\end{aligned} \tag{5.2}$$

5.2. Numerical Simulation

Numerical simulation of the CPWPM system with the above specific parameters is carried out in Simulink. Simulated signals in the time domain of the modulator within the duration

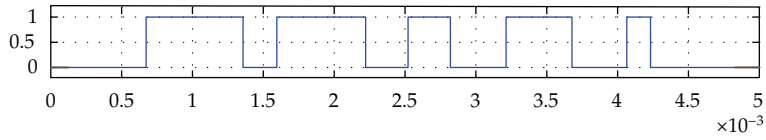

(a) Data_1

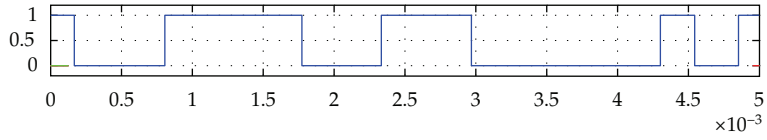

(b) Data_2

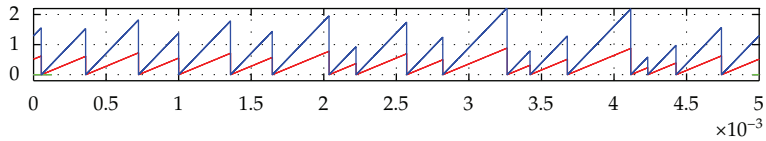

(c) Output signals of the counter (red) and the amplifier (blue)

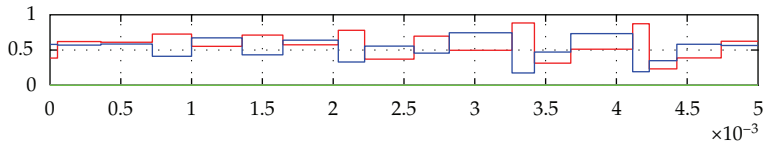

(d) Input (red) and output (blue) signals of the nonlinear converter $F(\cdot)$

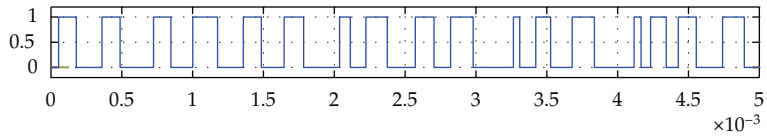

(e) CPWPM signal

Figure 7: Time-domain signals of the CPWPM modulator.

from starting time 0 to 5000 μs are presented in Figure 7. The intervals of position and width vary chaotically in the ranges 200 μs to 500 μs and 75 μs to 200 μs, respectively. When the synchronization state of the system is maintained, the recovered signals in the demodulator exactly match their corresponding signals in the modulator. The chaotic behavior of the system is verified by attractor diagram in Figure 8. In the modulation process, the fixed point is shifted on the bisector and around the average fixed point, $(X_{\text{av}}^1, X_{\text{av}}^2)$ (red point). Average spectrum of the CPWPM signal is shown in Figure 9. Values of the average fundamental harmonic and average bandwidth can be determined from this spectrum graph. We can observe that values of the average parameters in the simulation results are completely reasonable to that of the theoretical calculation above. This proves the validation of the theoretical analysis.

BER performance obtained from simulation of CPWPM, CPPM, PPM systems in the AWGN channel as well as the evaluation BER of the CPWPM system according to (3.4) is presented in Figure 10. Simulation BERs are calculated as the number of error bits divided

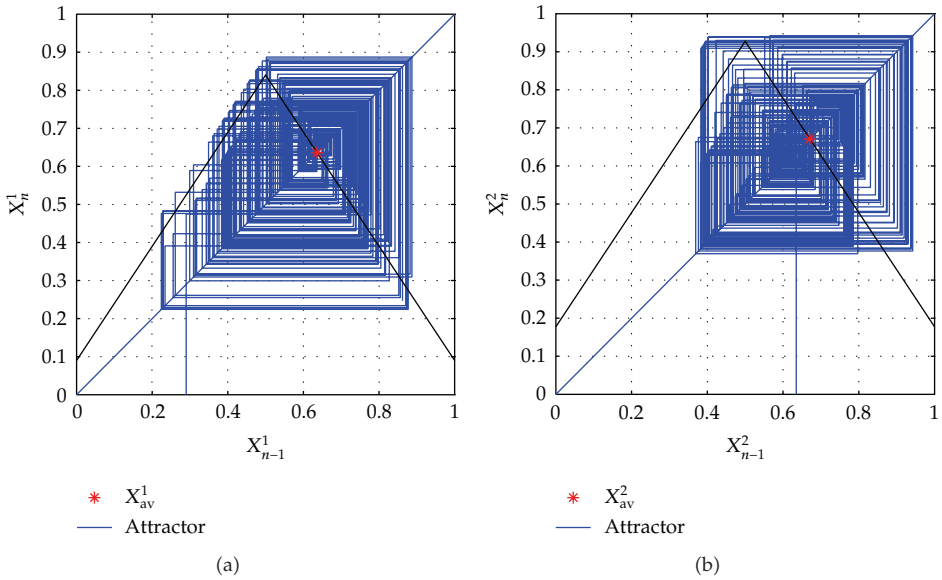

Figure 8: Attractor diagram with the average fixed point (X_{av}^1, X_{av}^2).

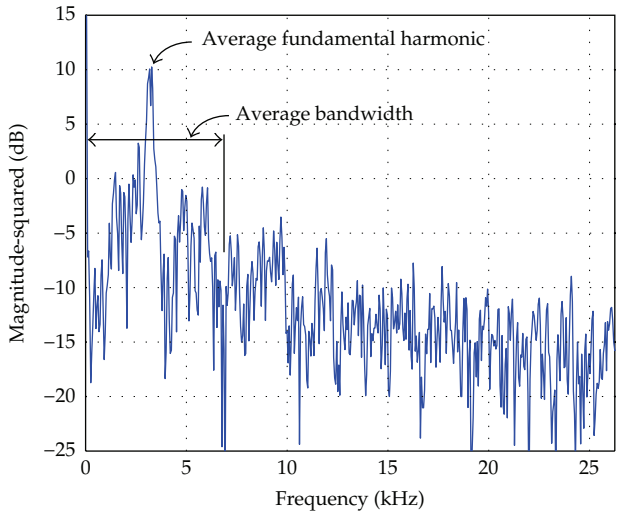

Figure 9: Average spectrum of the CPWPM signal.

by the total number of 10^8 bits transmitted. With the CPWPM system, the simulation BER is slightly higher than the evaluation one. The cause of these differences is the loss of synchronization. In the theoretical estimation, we suppose that the synchronization state is maintained at all times, thus errors in position and width of pulses leading to bit error only occur due to noise. However, in the numerical simulation, the effect of noise may cause not only the errors in position and width of pulses, but also the loss of synchronization which also leads to bit error. It can be observed that as the E_b/N_o increases, the synchronization of the system becomes better and thus the simulation results move closer to the estimation results.

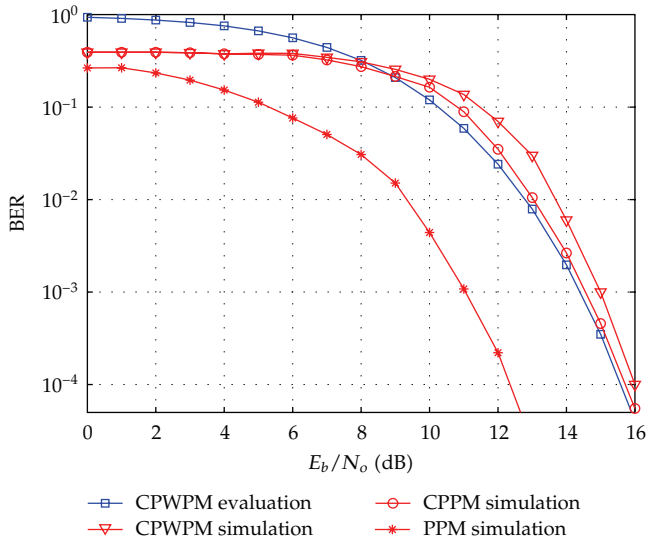

Figure 10: BER performance of CPWPM, CPPM, PPM systems in the AWGN channel.

Both BER performances of the CPWPM and CPPM systems are about 4 dB poorer than that of the conventional PPM system. This is due to simple demodulation of PPM, in which the information recovery does not depend on previous received intervals, data bit is determined by comparing current interval with a reference interval. The BER simulation results also point out that the CPWPM system performs slightly worse than the CPPM system, but in return the bit rate of the CPWPM system is twice as high as that of the CPPM system with equivalent parameters.

6. Conclusion

The paper has presented and investigated the chaotic-pulse-position-width modulation method for chaos-based digital communication. The performance of the method is analyzed using both theoretical evaluation and numerical simulation in terms of time- and frequency-domain signals and BER performance. In addition, the chaotic behavior of CPWPM with tent map is investigated considering the determination of the average parameters of the system in the modulation process. It can be seen from obtained results that: (1) the CPWPM system provides a significant improvement of bit rate with a slightly worse performance in comparison with an equivalent CPPM system; (2) two separate data streams can be conveyed by the CPWPM pulses and they are recovered separately at two corresponding outputs in the demodulator, thus CPWPM can be used as a multiaccess method of two users; (3) about the privacy, the CPWPM method offers an improvement compared with CPPM and a strong improvement compared with the PPM and PWM. Due to the chaotically-varied intervals of both the position and width, the CPWPM method can eliminate any trace of periodicity from the spectrum of the transmitted signal. Moreover, the chaotic variation depends on the privacy key with several parameters. It is impossible for an intruder to recover correctly the binary data without having full information on the structure of modulation and the private key; (4) the CPWPM pulses can be considered as a time-modulated baseband binary signal

and thus it can be conveyed by conventional binary sinusoidal carrier modulation methods such as on-off keying (OOK), binary-frequency-shift keying (BFSK) and binary-phase-shift keying (BPSK). All these features make the CPWPM method attractive for development of chaos-based digital communications.

Acknowledgment

This work is supported by the Vietnam's National Foundation for Science and Technology Development (NAFOSTED) under Grant no. 102.99-2010.17.

References

[1] S. H. Strogatz, *Nonlinear Dynamics And Chaos: With Applications To Physics, Biology, Chemistry, And Engineering*, Westview Press, Boulder, Colo, USA, 2001.
[2] M. P. Kennedy and G. Kolumban, "Special issue on non-coherent chaotic communications," *IEEE Transactions on Circuits and Systems I*, vol. 47, no. 12, pp. 1661–1764, 2000.
[3] P. Stavroulakis, *Chaos Applications in Telecommunications*, CRC Press, New York, NY, USA, 2005.
[4] W. M. Tam, F. C. M. Lau, and C. K. Tse, *Digital Communication with Chaos Multiple Access Techniques and Performance*, Elsevier Science, Amsterdam, The Netherlands, 2006.
[5] L. M. Pecora and T. L. Carroll, "Synchronization in chaotic systems," *Physical Review Letters*, vol. 64, no. 8, pp. 821–824, 1990.
[6] N. F. Rulkov and L. S. Tsimring, "Synchronization methods for communication with chaos over band-limited channels," *International Journal of Circuit Theory and Applications*, vol. 27, no. 6, pp. 555–567, 1999.
[7] C. C. Chen and K. Yao, "Numerical evaluation of error probabilities of self-synchronizing chaotic communications," *IEEE Communications Letters*, vol. 4, no. 2, pp. 37–39, 2000.
[8] M. M. Levy, "Some theoretical and practical considerations of pulse modulation," *Journal of the Institution of Electrical Engineerings*, vol. 94, no. 13, pp. 565–572, 1947.
[9] B. Wilson and Z. Ghassemlooy, "Pulse time modulation techniques for optical communications," *IEE Proceedings Optoelectronics*, vol. 140, no. 6, pp. 347–357, 1993.
[10] M. M. Sushchik, N. Rulkov, L. Larson et al., "Chaotic pulse position modulation: a robust method of communicating with chaos," *IEEE Communication Letters*, vol. 4, no. 4, pp. 128–130, 2000.
[11] N. F. Rulkov, M. M. Sushchik, L. S. Tsimring, and A. R. Volkovskii, "Digital communication using chaotic-pulse-position modulation," *IEEE Transactions on Circuits and Systems*, vol. 48, no. 12, pp. 1436–1444, 2001.
[12] H. Torikai, T. Saito, and W. Schwarz, "Synchronization via multiplex pulse trains," *IEEE Transactions on Circuits and Systems I*, vol. 46, no. 9, pp. 1072–1085, 1999.
[13] J. T. Bean and P. J. Langlois, "Current mode analog circuit for tent maps using piecewise linear functions," in *Proceedings of the 1994 IEEE International Symposium on Circuits and Systems*, vol. 6, pp. 125–128, June 1994.
[14] T. Addabbo, M. Alioto, A. Fort, S. Rocchi, and V. Vignoli, "The digital tent map: performance analysis and optimized design as a low-complexity source of pseudorandom bits," *IEEE Transactions on Instrumentation and Measurement*, vol. 55, no. 5, pp. 1451–1458, 2006.
[15] H. Ruan, E. E. Yaz, T. Zhai, and Y. I. Yaz, "A generalization of tent map and its use in EKF based chaotic parameter modulation/demodulation," in *Proceedings of the 43rd IEEE Conference on Decision and Control (CDC '04)*, vol. 2, pp. 2071–2075, December 2004.